Powder X-ray diffraction of nintedanib esylate hemihydrate, $(C_{31}H_{33}N_5O_4)(C_2H_5O_3S)(H_2O)_{0.5}$

Tawnee M. Ens,[1] James A. Kaduk,[2,3,a)] Anja Dosen,[4] and Thomas N. Blanton[4]
[1]*North Central College, 131 S. Loomis St., Naperville, IL 60540, USA*
[2]*Illinois Institute of Technology, 3101 S. Dearborn St., Chicago, IL 60616, USA*
[3]*North Central College, 131 S. Loomis St., Naperville, IL 60540, USA*
[4]*ICDD, 12 Campus Blvd., Newtown Square, PA 19073-3273, USA*

(Received 19 January 2024; accepted 21 March 2024)

The crystal structure of nintedanib esylate hemihydrate was refined using synchrotron X-ray powder diffraction data and optimized using density functional theory techniques. Nintedanib esylate hemihydrate crystallizes in space group *P-1* (#2) with $a = 11.5137(1)$, $b = 16.3208(4)$, $c = 19.1780(5)$ Å, $\alpha = 69.0259(12)$, $\beta = 84.4955(8)$, $\gamma = 89.8319(6)°$, $V = 3347.57(3)$ Å^3, and $Z = 4$ at 295 K. Hydrogen bonds are prominent in the crystal structure. The water molecule forms two medium-strength O–H···O hydrogen bonds to one of the esylate anions. The protonated nitrogen atom in each cation forms a N–H···O hydrogen bond to an esylate anion. The ring N–H groups form strong intramolecular N–H···O hydrogen bonds to carbonyl groups. The ring N–H groups form intramolecular N–H···O hydrogen bonds to esylate anions. Many C–H···O hydrogen bonds (and one C–H···N hydrogen bond), with aromatic C–H, methylene groups and methyl groups as donors, are present. The hydrogen bonding patterns of the two cations differ considerably. The powder pattern has been submitted to ICDD for inclusion in the Powder Diffraction File™ (PDF®)

[doi:10.1017/S0885715624000186]

Keywords: nintedanib esylate hemihydrate, Ofev, powder diffraction, rietveld refinement, density functional theory

Nintedanib (free base CAS Registry Number 656247-17-5) is a drug for the treatment of idiopathic pulmonary fibrosis (IPF) as well as non-small cell lung cancer (NSCLC). In NSCLC, Nintedanib (brand name Vargatef) inhibits three types of growth factor receptors that are involved in angiogenesis for tumor growth as an inhibitor of tyrosine kinases (Yan et al., 2023). In IPF, Nintedanib (brand name Ofev) has antifibrotic properties involving growth factors in the lungs that act against connective tissue formation by inhibiting fibroblast proliferation, which acts similarly to its tumor inhibition properties (Wollin et al., 2015; Marijic et al., 2021). Nintedanib is FDA-approved for Ofev, as an IPF treatment, that has been proven to reduce significant cell proliferation in the lungs against IPF and has been recognized to work well against NSCLC and systemic sclerosis by delaying long-term proliferation. Hepatotoxicity due to increased liver enzymes in metabolism is the main drawback of this type of therapy but has otherwise had promising results for IPF and NSCLC (Gole and Bankole, 2023).

Primarily administered in a salt form as nintedanib esylate (Figure 1 inset, CAS Registry Number 656247-18-6), the systematic name is methyl (3Z)-3-(((4-(N-methyl-2-(4-methylpiperazin-1-yl)acetamido)phenyl)amino) (phenyl)methylidene)-2-oxo-2,3-dihydro-1H-indole-6-carboxylate ethanesulfonate. This work was carried out as part of a project to determine the crystal structures of large-volume commercial pharmaceuticals and include high-quality powder diffraction data for them in the Powder Diffraction File (Gates-Rector and Blanton, 2019).

The synchrotron pattern (Figure 1) of a commercial reagent (purchased from TargetMol, lot #131360) was measured at 11-BM at APS (Antao et al., 2008; Lee et al., 2008; Wang et al., 2008) using a wavelength of 0.459744 Å). The pattern was indexed using N-TREOR (Altomare et al., 2013) on a primitive triclinic unit cell. Triclinic lattice parameters for nintedanib esylate hemihydrate, CAS Registry Number 959762-24-4 (space group *P-1*, which had a similar unit cell) and a powder pattern were reported by Roth et al. (2006; Boehringer Ingelheim Pharma GmbH), but no atom coordinates were included. A connectivity search in the Cambridge Structural Database (Groom et al., 2016) yielded the Refcode YASMIS for nintedanib esylate hemihydrate (Ma et al., 2022). Although purchased as anhydrous, the sample seems to be the hemihydrate. The sample contains an unknown crystalline impurity. Thirteen peaks from this phase could be indexed on a primitive monoclinic unit cell

a)Author to whom correspondence should be addressed. Electronic mail: kaduk@polycrystallography.com

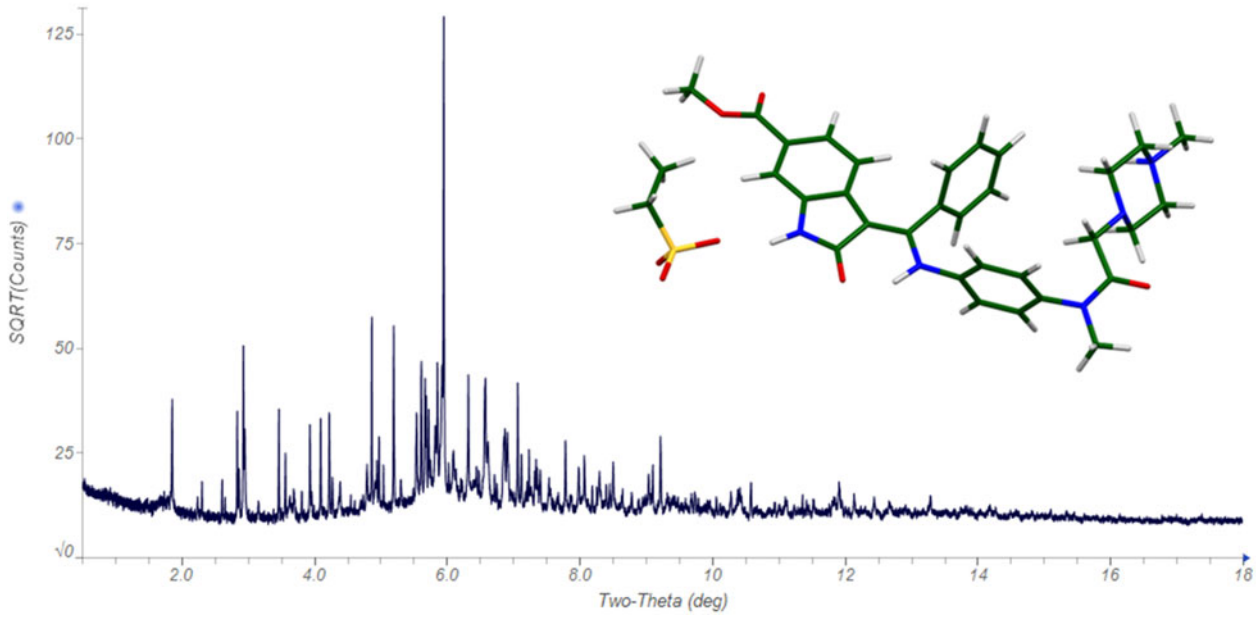

Figure 1. Nintedanib esylate hemihydrate synchrotron X-ray diffraction pattern. Inset nintedanib esylate hemihydrate molecule. Image generated using JADE Pro (MDI, 2024) and Mercury (Macrae et al., 2020).

having $a = 14.2907$, $b = 4.6233$, $c = 23.6130$ Å, $\beta = 91.779°$, and $V = 1559.37$ Å^3; this impurity phase was included in the refinement as a Le Bail phase. The structure of the nintedanib esylate hemihydrate phase was refined using GSAS-II (Toby and Von Dreele, 2013) using an ordered model (removing a minor orientation of one of the esylate anions) and optimized using VASP (Kresse and Furthmüller, 1996). A single-point density functional calculation (fixed experimental cell) and population analysis were carried out using CRYSTAL23 (Erba et al., 2022).

The crystal structure contains corrugated layers parallel to the *bc*-plane. Our lattice parameters (Table I) fall between those of the other two determinations; perhaps, the water content varies among samples. Hydrogen bonds (Table II) are prominent in the crystal structure. The water molecule O13 forms two medium-strength O–H···O hydrogen bonds to one of the esylate anions. The protonated nitrogen atom in each cation forms an N–H···O hydrogen bond to an esylate anion. The ring N–H groups N31 and N102 form strong intramolecular N–H···O hydrogen bonds to carbonyl groups. The ring N–H groups N24 and N104 form intramolecular N–H···O hydrogen bonds to esylate anions. Many C–H···O hydrogen bonds (and one C–H···N hydrogen bond), with aromatic C–H, methylene groups, and methyl groups as donors are present. The hydrogen bonding patterns of the two cations differ considerably. A Mogul geometry analysis indicates that torsion angles involving rotation about the C43–N31 bond are unusual; these fall in a valley in a very broad distribution, so, perhaps, the intramolecular hydrogen bond has resulted in an unusual conformation. The C119–C115 torsion angles are also flagged as unusual.

TABLE I. Reduced lattice parameters of nintedanib esylate hemihydrate. Space group *P-1*

Source	US 7,119,093	YASMIS	This Work
Temperature, K	ambient?	293	295
a, Å	11.503	11.4908(8)	11.5137(1)
b, Å	16.332	16.2382(12)	16.3208(4)
c, Å	19.199	19.1538(14)	19.1780(5)
α,°	69.17	69.142(4)	69.0259(12)
β,°	84.73	84.616(3)	84.4955(8)
γ,°	89.87	89.777(4)	89.8319(6)
V, Å^3	3354.4	3323.28	3347.57(3)

I. DEPOSITED DATA

The powder pattern of nintedanib esylate hemihydrate from this synchrotron data set has been submitted to ICDD for inclusion in the Powder Diffraction File. The Crystallographic Information Framework (CIF) files containing the results of the Rietveld refinement (including the raw data) and the DFT geometry optimization were deposited with the ICDD. The data can be requested at pdj@icdd.com.

ACKNOWLEDGEMENTS

The use of the Advanced Photon Source at Argonne National Laboratory was supported by the U. S. Department of Energy, Office of Science, Office of Basic Energy Sciences, under Contract No. DE-AC02-06CH11357. This work was partially supported by the International Centre for Diffraction Data. We thank Saul Lapidus for his assistance in the data collection.

CONFLICTS OF INTEREST

The authors have no conflicts of interest to declare.

https://doi.org/10.1017/S0885715624000186 Published online by Cambridge University Press

TABLE II. Hydrogen bonds (CRYSTAL23) in nintedanib esylate hemihydrate

H-Bond	D–H, Å	H···A, Å	D···A, Å	D–H···A,◦	Overlap, *e*	*E*, kcal/mol
O13–H14···O17	0.993	1.771	2.755	170.6	0.048	12.0
O13–H15···O18	0.995	1.752	2.740	171.5	0.059	13.3
N29–H30···O13	1.076	1.652	2.716	169.2	0.099	7.3
N100–H101···O4	1.064	1.647	2.686	164.1	0.082	6.6
N31–H32···O23	1.046	1.766[a]	2.671	112.2	0.079	6.5
N102–H103···O99	1.047	1.731[a]	2.654	144.5	0.083	6.6
N24–H25···O3	1.030	1.840	2.808	155.1	0.064	5.8
N104–H105···O17	1.024	1.988	2.923	150.5	0.045	4.9
C54–H55···O26	1.090	2.479	3.276	128.9	0.012	
C67–H68···O23	1.091	2.565	3.366	129.5	0.011	
C146–H147···O26	1.089	2.586	3.332	124.9	0.012	
C158–H159···O2	1.092	2.246	3.290	159.3	0.032	
C160–H161···O98	1.091	2.604	3.600	151.4	0.013	
C50–H51···O3	1.100	2.653	3.743	170.8	0.017	
C111–H112···O98	1.099	2.578[a]	3.270	120.1	0.010	
C62–H63···O16	1.095	2.233	3.163	141.4	0.018	
C86–H87···O98	1.099	2.334	3.359	154.5	0.021	
C133–H139···O33	1.095	2.279	2.961	118.4	0.016	
C131–H132···O16	1.100	2.486	3.472	148.6	0.016	
C131–H133···O2	1.098	2.444	3.369	141.0	0.017	
C138–H140···O16	1.096	2.585	3.542	145.4	0.012	
C82–H84···O18	1.097	2.480	3.531	159.7	0.018	
C82–H85···O98	1.095	2.579	3.523	143.8	0.012	
C150–H151···O16	1.097	2.517	3.476	145.3	0.014	
C150—H152···O23	1.098	2.389	3.431	157.7	0.024	
C150–H153···O2	1.094	2.455	3.404	144.2	0.011	
C150–H153···O3	1.094	2.366	3.345	148.0	0.017	
C93–H95···O33	1.094	2.284	2.766	104.3	0.022	
C19–H171···N97	1.101	2.857	3.423	146.8	0.015	
C22–H173···O124	1.097	2.586	3.827	132.4	0.010	

[a]Intramolecular.

REFERENCES

Altomare, A., C. Cuocci, C. Giacovazzo, A. Moliterni, R. Rizzi, N. Corriero, and A. Falcicchio. 2013. "EXPO2013: A Kit of Tools for Phasing Crystal Structures from Powder Data." *Journal of Applied Crystallography* 46: 1231–5.

Antao, S. M., I. Hassan, J. Wang, P. L. Lee, and B. H. Toby. 2008. "State-of-the-Art High-Resolution Powder X-ray Diffraction (HRPXRD) Illustrated with Rietveld Refinement of Quartz, Sodalite, Tremolite, and Meionite." *Canadian Mineralogist* 46: 1501–9.

Erba, A., J. K. Desmaris, S. Casassa, B. Civalleri, L. Donà, I. J. Bush, B. Searle, L. Maschio, L.-E. Daga, A. Cossard, C. Ribaldone, E. Ascrizzi, N. L. Marana, J.-P. Flament, and B. Kirtman. 2022. "CRYSTAL23: A Program for Computational Solid State Physics and Chemistry." *Journal of Chemical Theory and Computation* 19: 6891–932. doi:10.1021/acs.jctc.2c00958.

Gates-Rector, S., and T. N. Blanton. 2019. "The Powder Diffraction File: A Quality Materials Characterization Database." *Powder Diffraction* 39: 352–60.

Gole, S. & A. Bankole. 2023. Nintedanib – StatPearls – NCBI Bookshelf. www.ncbi.nlm.nih.gov/books/NBK585049/.

Groom, C. R., I. J. Bruno, M. P. Lightfoot, and S. C. Ward. 2016. "The Cambridge Structural Database." *Acta Crystallographica Section B: Structural Science, Crystal Engineering and Materials* 72: 171–9.

Kresse, G., and J. Furthmüller. 1996. "Efficiency of Ab-Initio Total Energy Calculations for Metals and Semiconductors Using a Plane-Wave Basis Set." *Computational Materials Science* 6: 15–50.

Lee, P. L., D. Shu, M. Ramanathan, C. Preissner, J. Wang, M. A. Beno, R. B. Von Dreele, L. Ribaud, C. Kurtz, S. M. Antao, X. Jiao, and B. H. Toby. 2008. "A Twelve-Analyzer Detector System for High-Resolution Powder Diffraction." *Journal of Synchrotron Radiation* 15: 427–32.

Ma, J., J. Huang, Z. Cao, J. Sha, R. Sun, H. He, Y. Wan, Y. Li, T. Li, and B. Ren. 2022. "Solubility Measurement and Thermodynamic Properties of Nintedanib Esylate Hemihydrate in Pure Solvents." *Journal of Molecular Liquids* 352: 118624.

Macrae, C. F., I. Sovago, S. J. Cottrell, P. T. A. Galek, P. McCabe, E. Pidcock, M. Platings, G. P. Shields, J. S. Stevens, M. Towler, and P. A. Wood. 2020. "Mercury 4.0: From Visualization to Design and Prediction." *Journal of Applied Crystallography* 53: 226–35.

Marijic, P., L. Schwarzkopf, L. Schwettmann, T. Ruhnke, F. Trudzinski, and M. Kreuter. 2021. "Pirfenidone vs. Nintedanib in Patients with Idiopathic Pulmonary Fibrosis: A Retrospective Cohort Study." *Respiration Research* 22: 1–11. doi:10.1186/s12931-021-01857-y.

MDI (2024). *JADE Pro version 9.0* (Materials Data, Livermore, CA).

Roth, G. K., G. Linz, P. Sieger, W. Rall, F. Hilberg, & T. Bock. 2006. "3-Z-[1-(4-(N-((4-Methyl-Piperazin-1-yl)Methylcarbonyl)-N-Methylamino) Anilino)-1-Phenylmethylene]-6-Methoxycarbonyl-2-Indolinone Monoethanesulfonate and the Use Thereof as a Pharmaceutical Composition." United States Patent 7,119,093 B2 (Boehringer Ingelheim Pharma GmbH).

Toby, B. H., and R. B. Von Dreele. 2013. "GSAS II: The Genesis of a Modern Open Source All Purpose Crystallography Software Package." *Journal of Applied Crystallography* 46: 544–9.

Wang, J., B. H. Toby, P. L. Lee, L. Ribaud, S. M. Antao, C. Kurtz, M. Ramanathan, R. B. Von Dreele, and M. A. Beno. 2008. "A Dedicated Powder Diffraction Beamline at the Advanced Photon Source: Commissioning and Early Operational Results." *Review of Scientific Instruments* 79: 085105.

Wollin, L., E. Wex, A. Pautsch, G. Schnapp, K. E. Hostettler, S. Stowasser, and M. Kolb. 2015. "Mode of Action of Nintedanib in the Treatment of Idiopathic Pulmonary Fibrosis." *European Respiratory Journal* 45: 1434–45. doi:10.1183/09031936.00174914.

Yan, S., S. Xue, T. Wang, R. Gao, H. Zeng, Q. Wang, and X. Jia. 2023. "Efficacy and Safety of Nintedanib in Patients with Non-Small Cell Lung Cancer, and Novel Insights in Radiation-Induced Lung Toxicity." *Frontiers in Oncology* 13: 1086214. doi:10.3389/fonc.2023.1086214.

https://doi.org/10.1017/S0885715624000186 Published online by Cambridge University Press